Project Report
TIP-76

Development of a Built-In, Metal-Air, Hydrogen Nanobattery: FY18 Energy Technical Investment Program

A.C. Weathers
R.O. Ouedraogo
G. Beach
A.J. Tan
S. Sheffels

7 December 2018

Lincoln Laboratory
MASSACHUSETTS INSTITUTE OF TECHNOLOGY
LEXINGTON, MASSACHUSETTS

This material is based upon work supported by the Assistant Secretary of Defense for Research and Engineering under Air Force Contract No. FA8702-15-D-0001.

DISTRIBUTION STATEMENT A. Approved for public release. Distribution is unlimited.

This report is the result of studies performed at Lincoln Laboratory, a federally funded research and development center operated by Massachusetts Institute of Technology. This material is based upon work supported by the Assistant Secretary of Defense for Research and Engineering under Air Force Contract No. FA8702-15-D-0001. Any opinions, findings and conclusions or recommendations expressed in this material are those of the authors and do not necessarily reflect the views of the Assistant Secretary of Defense for Research and Engineering.

© 2018 MASSACHUSETTS INSTITUTE OF TECHNOLOGY

Delivered to the U.S. Government with Unlimited Rights, as defined in DFARS Part 252.227-7013 or 7014 (Feb 2014). Notwithstanding any copyright notice, U.S. Government rights in this work are defined by DFARS 252.227-7013 or DFARS 252.227-7014 as detailed above. Use of this work other than as specifically authorized by the U.S. Government may violate any copyrights that exist in this work.

Massachusetts Institute of Technology
Lincoln Laboratory

Development of a Built-In, Metal-Air, Hydrogen Nanobattery:
FY18 Energy Technical Investment Program

A.C. Weathers
Group 81

R.O. Ouedraogo
Group 92

G. Beach
A.J. Tan
S. Sheffels
MIT

Project Report TIP-76

7 December 2018

DISTRIBUTION STATEMENT A. Approved for public release. Distribution is unlimited.

Lexington Massachusetts

1. INTRODUCTION AND MOTIVATION

High-capacity batteries that are ubiquitous in consumer electronics contain rigid and thick substrates to accommodate high temperature material processing, bulky packaging to contain liquid electrolytes, and generally cannot be scaled to micron scale dimensions. Even thin-film solid-state lithium ion batteries require the use of ~100 μm thick support material composed of silicon or metal, which limits the effective energy density and ability to scale to sub-micron dimensions. As a result, the realization of micro- or nano-scale batteries that can provide localized power distribution within an integrated circuit (IC) or low-power sensors has remained impractical. As an alternative, we have developed a hydrogen nanobattery composed of materials that can easily be scaled to nanometer-scale device thickness, can be patterned to micron- or nanometer-scale lateral dimensions, and can be deposited at room temperature for integration with thin polymer support substrates or with back-end-of-line (BEOL) microelectronics processing.

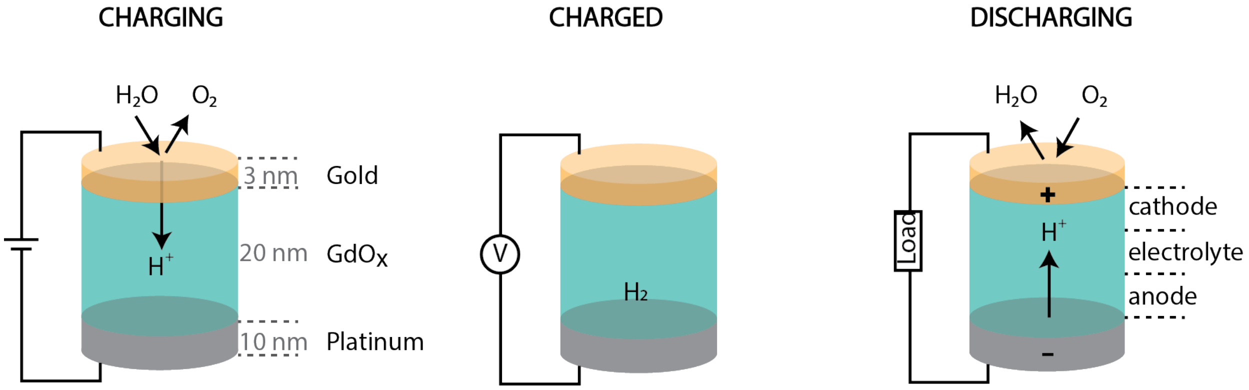

Figure 1. Schematic of the device layout and charging and discharging mechanisms of the GdO_x hydrogen nanobattery.

The hydrogen nanobattery is composed of a platinum current collector, a gadolinium oxide (GdO_x) active layer, and a 3 nm gold catalyst electrode, as shown in Figure 1, that are all radio-frequency (RF) sputtered at room temperature. Like other solid-oxide electrolysis cells (SOECs), energy is stored in the hydrogen ions that are produced by an electrolysis reaction at the gold surface electrode during charging, and that are driven into the GdO_x film as a result of the applied voltage. Upon discharging, hydrogen ions flow across the GdO_x electrolyte, while electrons simultaneously flow through an external load, and recombine at the gold/GdO_x interface with oxygen molecules to produce water vapor. Because of the fast kinetics of hydrogen diffusion and storage, we have found that thin-film GdO_x SOECs have two orders of magnitude larger power density (Figure 2) compared to typical lithium-ion batteries, which require lithium ion diffusion and intercalation. Furthermore, because the nanobattery generates and stores interstitial hydrogen from the water splitting reaction at *room-temperature*, this system offers an attractive alternative to traditional SOECs based on ZrO_2 that typically operate close to 1000°C. [1]

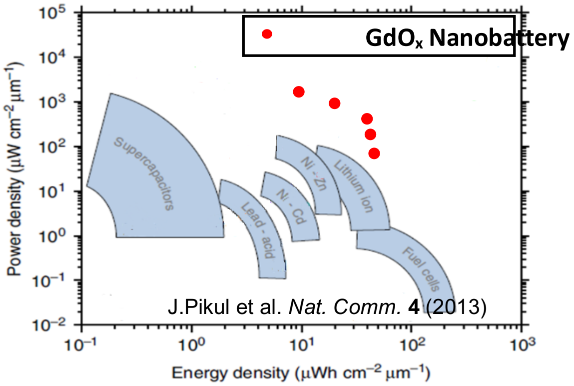

Figure 2. Comparison of volumetric energy and power densities of common battery technologies in comparison with the gadolinium oxide (GdO$_x$) nanobattery.

2. METAL OXIDE STRUCTURE-PROPERTY RELATIONSHIP

To optimize the metal oxide functional layer in our device, we have tested a number of other metal oxides including yttrium oxide (YO_x), zirconium oxide (ZrO_x) and tantalum oxide (TaO_x) to determine whether the performance of GdO_x is unique to its chemical and crystal structure. These compounds were chosen based on the fact that they are all high-k binary oxides, like GdO_x, but with a variety of crystal structures and basicity, a measure of an oxide's tendency to react with water to produce hydroxide (-OH) compounds. As shown in Figure 3, only bixbyite structured basic oxides appear to exhibit electrolysis behavior in the presence of a gold catalytic electrode, suggesting the importance of hydroxide defects in providing a hopping pathway for hydrogen ions in the electrolyte.

To confirm the crystal structure of the GdOx nanobattery and investigate the film morphology, we performed transmission electron microscopy (TEM) analysis of the GdOx film. Figure 4 shows the darkfield, brightfield, and selected area diffraction (SAD) pattern of a 50 nm thick GdOx film. The darkfield image in Figure 4a highlights the nanometer scale grain size, which could be an important parameter if hydrogen diffusion is concentrated along grain boundaries. The SAD pattern in Figure 4b can mostly be indexed to polycrystalline Gd_2O_3, although the presence of other phases such as $Gd(OH)_3$, likely co-exist.

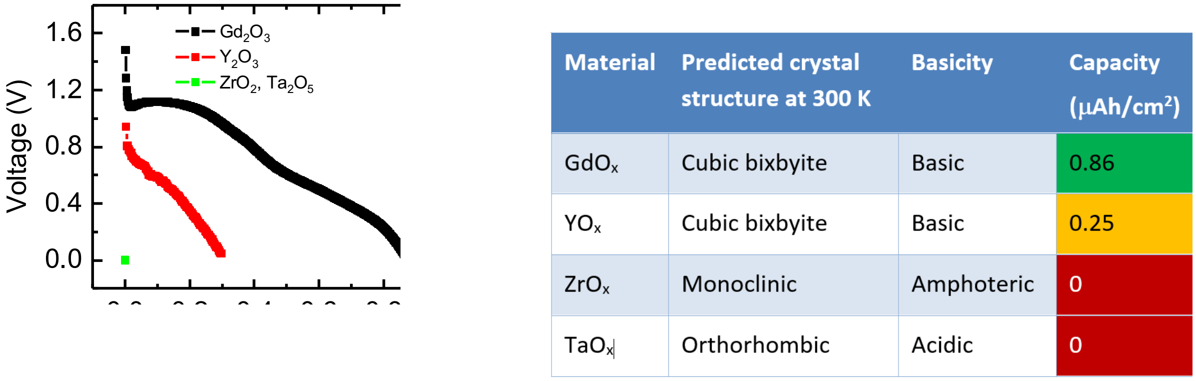

Material	Predicted crystal structure at 300 K	Basicity	Capacity (μAh/cm^2)
GdO_x	Cubic bixbyite	Basic	0.86
YO_x	Cubic bixbyite	Basic	0.25
ZrO_x	Monoclinic	Amphoteric	0
TaO_x	Orthorhombic	Acidic	0

Figure 3. Performance of thin-film solid-oxide electrolysis cell (SOEC) comprised of different solid-oxides, with a range of crystal structures and basicity.

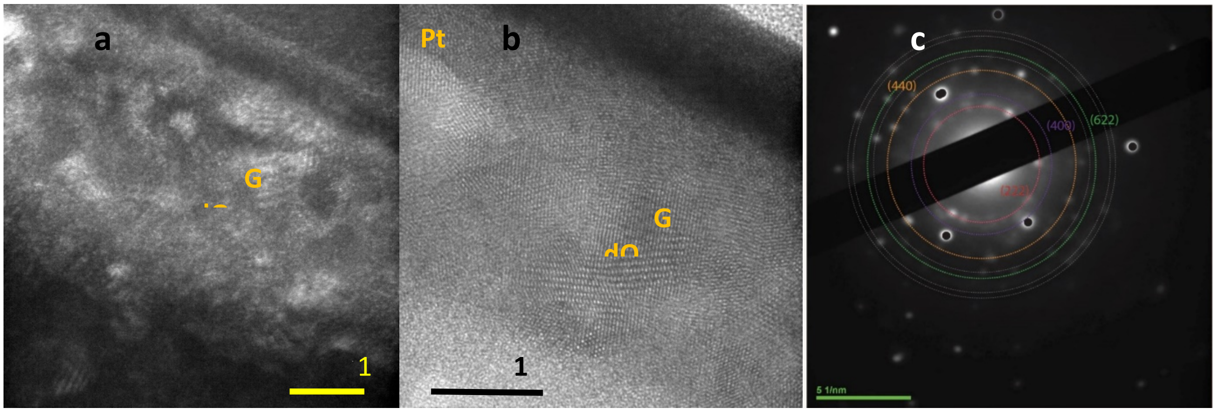

Figure 4. Transmission electron microscopy (TEM) (a) darkfield and (b) brightfield images indicating nanometer scale GdO_x grain size. (c) The selected area diffraction (SAD) pattern of the GdOx film can mostly be indexed to the cubic bixbyite phase of GdO_x, although other structural phases are likely present.

3. CYCLABILITY

While FY17 focused on determining the operational mechanism of the battery, FY18 has been focused on optimization of device performance. Namely, the cyclability has been improved by decreasing the charging voltage from 3 V to 2 V, but extending the charging time from 10 minutes to 20 minutes. Under these conditions, devices have been found to cycle for as many as 80 cycles before failing (Figure 5), with consistent voltage discharge curves with a nominal voltage plateau around 0.6 V.

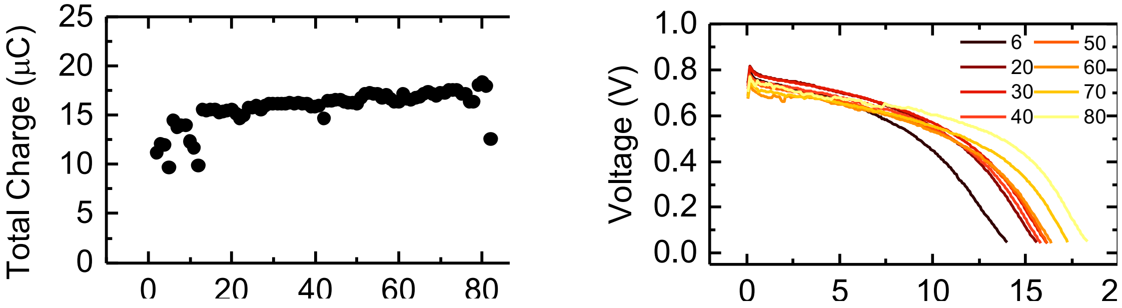

Figure 5. (left) Capacity and (right) discharge curve of a hydrogen nanobattery under optimal charging conditions of +2 V over 20 minutes. The capacity shows excellent capability, and the discharge curve shows a consistent voltage plateau.

4. SCALABILITY

Processes improvements in the RF sputtering deposition parameters, i.e., deposition pressure and rotation speed, have allowed us to largely overcome pinhole defects, which has enables us to demonstrate two orders of magnitude lateral device scaling, from ~100 μm diameter devices to millimeter scale. Figure 6 shows an example of 1 and 4 mm^2 devices that indicate the expected linear trend in capacity and power with lateral area. Figure 7 shows the discharge curve of two representative devices with 1 mm^2 and 4 mm^2 lateral area, indicating comparable performance. The use of a sputter system with a larger deposition target would enable larger device fabrication.

In addition to demonstrating reasonable lateral scalability, we have also demonstrated patterning to micron scale dimensions using standard lithography processes to produce battery strips along a silicon wafer, shown in Figure 6. The ~10 nm scale thickness of the device allows for straightforward patterning to nanometer scale dimensions, provided the lithography resolution.

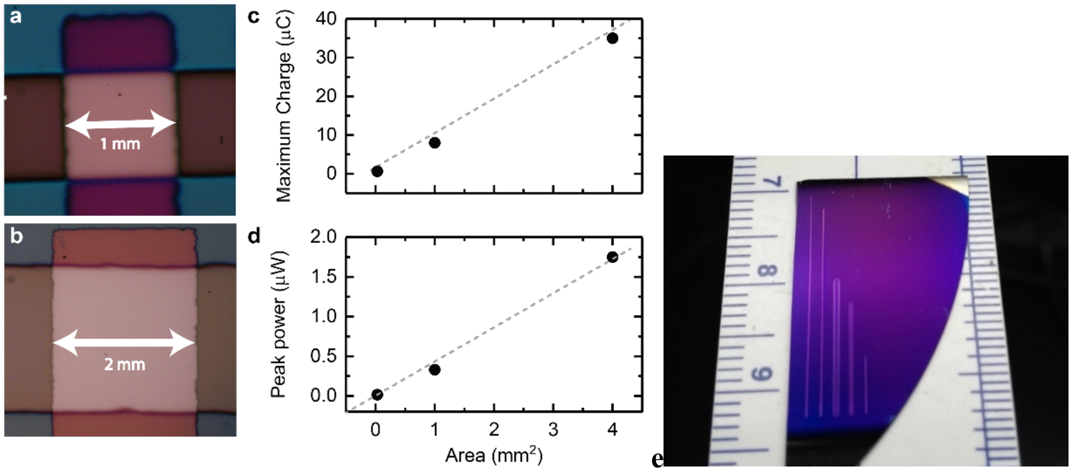

Figure 6. Image of (a) 1 mm^2 and (b) 4 mm^2 hydrogen nanobattery and the corresponding (c) capacity and (d) peak power showing the linear scaling with area. (e) Demonstration of battery patterning to micron scale dimensions.

While the battery can be scaled laterally to produce larger capacity, the overall areal capacity and areal power density is low due to the very thin GdO_x functional region. For example, 50 nm thick devices have capacities on the order of 200 nW-hr/cm^2 and power densities of 50 μW/cm^2. However, we have found that increasing the thickness of the GdO_x has little effect on the overall areal capacity, as shown in Figure 8, for films between 20 and 120 nm. This plateau in the areal capacity is likely a result of the saturation of only a top ~20 nm of GdO_x with sufficient hydroxide defects to support hydrogen ion conduction and hydrogen storage.

In order to improve the thickness scaling we have experimented with hour- to day-long post-deposition hydration steam treatments in a temperature and humidity controlled chamber. Exposure of GdO_x to water is expected to cause a phase transition from the basic GdO_x oxide to $Gd(OH)_3$, providing additional conduction pathways for hydrogen ions. Figure 8 shows the impendence spectroscopy Nernst plots of a 50 nm thick GdOx device as deposited, and after 1 and 3 hour steam treatments. The reduction in the radius of the Nernst plot hemisphere indicates a reduction in the complex impedance and higher overall ionic resistance of the device following longer hydration treatments. As deposited, the device has an ionic resistance on the order of 100 MΩ, which is reduced to 10 and 0.1 MΩ after 1 and 3 hour treatments, respectively. This observation of increasing ionic conductivity with increasing exposure to water vapor supports our hypothesis that the capacity of the GdO_x functional layer is limited by the presence of hydroxide defects that provide a hopping conduction path for hydrogen ions. Further efforts in FY19 will explore whether this method can be used to produce thicker GDOx devices with improved areal capacity.

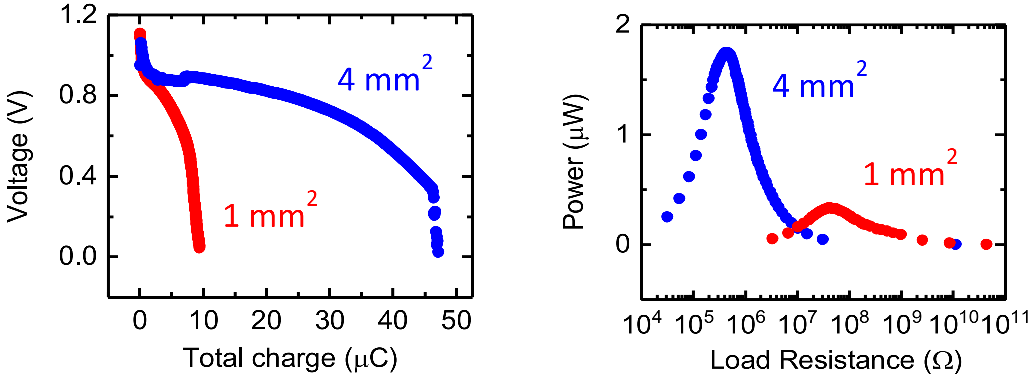

Figure 7. (left) Discharge curve of a 1 mm² (red) and 4 mm² (blue) GdOx nanobattery. (right) Power produced by the same devices as a function of load resistance.

5. FOLLOW-ON WORK

Follow-on work in FY19 will focus on elucidating the mechanism for improved ionic conductivity with post-deposition steam treatments, and whether this technique can provide an improvement in the areal capacity with thicker GdOx films. Following this investigation, we will demonstration a prototype system composed of a GdO_x nanobattery powering a low-power circuit.

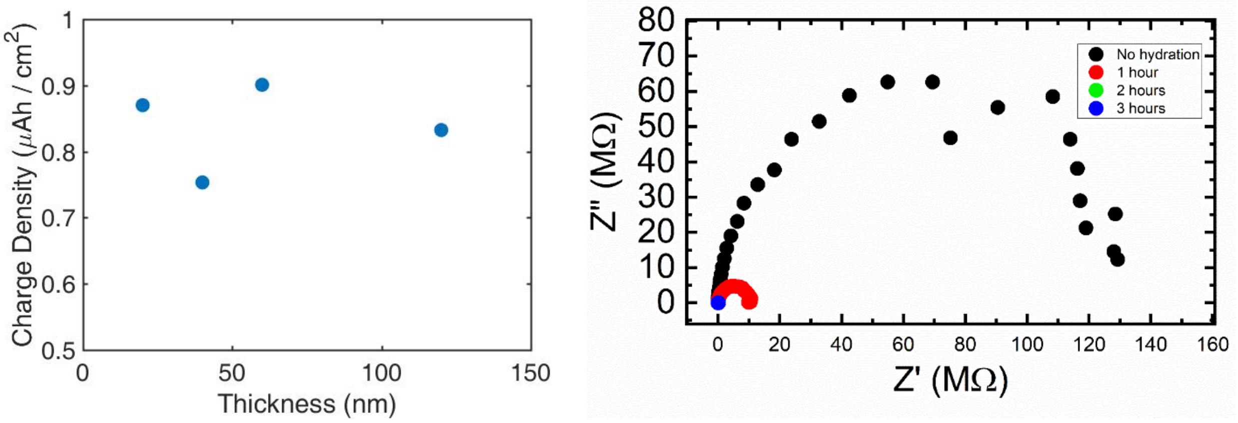

Figure 8. (left) Areal capacity for four different thicknesses of GdOx, indicating a plateau in the capacity beyond 20 nm. (right) Impedance spectroscopy Nernst plots of the complex impedance of a 50 nm device following hydration steam treatments. Smaller hemispheres indicate a lower impedance. The inset is a zoomed-in image of the blue curve (3-hour treatment).